J Biol Inorg Chem (2005) 10: 903–912
DOI 10.1007/s00775-005-0043-z

ORIGINAL ARTICLE

Won Bae Jeon · Steven W. Singer · Paul W. Ludden
Luis M. Rubio

New insights into the mechanism of nickel insertion into carbon monoxide dehydrogenase: analysis of *Rhodospirillum rubrum* carbon monoxide dehydrogenase variants with substituted ligands to the [Fe_3S_4] portion of the active-site C-cluster

Received: 5 August 2005 / Accepted: 3 October 2005 / Published online: 8 November 2005

Abstract Carbon monoxide dehydrogenase (CODH) from *Rhodospirillum rubrum* catalyzes the oxidation of CO to CO_2. A unique [$NiFe_4S_4$] cluster, known as the C-cluster, constitutes the active site of the enzyme. When grown in Ni-deficient medium *R. rubrum* accumulates a Ni-deficient apo form of CODH that is readily activated by Ni. It has been previously shown that activation of apo-CODH by Ni is a two-step process involving the rapid formation of an inactive apo-CODH•Ni complex prior to conversion to the active holo-CODH. We have generated CODH variants with substitutions in cysteine residues involved in the coordination of the [Fe_3S_4] portion of the C-cluster. Analysis of the variants suggests that the cysteine residues at positions 338, 451, and 481 are important for CO oxidation activity catalyzed by CODH but not for Ni binding to the C-cluster. C451S CODH is the only new variant that retains residual CO oxidation activity. Comparison of the kinetics and pH dependence of Ni activation of the apo forms of wild-type, C451S, and C531A CODH allowed us to develop a model for Ni insertion into the C-cluster of CODH in which Ni reversibly binds to the C-cluster and subsequently coordinates Cys531 in the rate-determining step.

Keywords Carbon monoxide dehydrogenase · Ni activation · *Rhodospirillum rubrum* · Electron paramagnetic resonance

W. B. Jeon
Center for Eukaryotic Structural Genomics,
Department of Biochemistry, University of Wisconsin-Madison,
Madison, WI 53706, USA

S. W. Singer · P. W. Ludden · L. M. Rubio (✉)
Department of Plant and Microbial Biology,
University of California-Berkeley,
111 Koshland Hall, Berkeley, CA 94720-3102, USA
E-mail: lrubio@nature.berkeley.edu
Tel.: +1-510-6433940
Fax: +1-510-6424995

Abbreviations CHES: 2-(Cyclohexylamino)ethanesulfonic acid · Apo-CODH: Ni-deficient carbon monoxide dehydrogenase · CODH: Carbon monoxide dehydrogenase · DEAE: (Diethylamino)ethyl · DTH: Sodium dithionite · EPR: Electron paramagnetic resonance · FCII: Ferrous component II site · K_D: Dissociation constant · k_{max}: Maximal rate constant for activation · k_{obs}: Apparent first-order rate constant · MES: 2-(*N*-Morpholino)ethanesulfonic acid · MN: Malate–ammonium · MOPS: 3-(*N*-Morpholino)propanesulfonate · SDS-PAGE: Sodium dodecyl sulfate polyacrylamide gel electrophoresis

Introduction

Carbon monoxide dehydrogenase (CODH) (EC 1.2.99.2) is a Ni-containing oxidoreductase that catalyzes the oxidation of CO to CO_2 in an overall reaction $CO + H_2O \leftrightarrow CO_2 + 2e^- + 2H^+$ ($\Delta G_o = -20$ kJ mol^{-1}) [1]. Ni-dependent carbon monoxide oxidation activity is widely distributed among archaea and bacteria. CODH isolated from the photosynthetic bacterium *Rhodospirillum rubrum* is a homodimer that contains an [Fe_4S_4] cluster (B-cluster) and an unusual [$NiFe_4S_4$] cluster (C-cluster) in each subunit; an additional [Fe_4S_4] cluster (D-cluster) bridges the two subunits [2]. Extensive evidence suggests oxidation of CO to CO_2 occurs at the C-cluster, and the B- and D-clusters mediate electron transfer from the C-cluster to the electron acceptor protein CooF [3]. CooF transfers electrons to a membrane-bound [NiFe] hydrogenase, which evolves H_2. The hydrogenase couples H_2 evolution and proton translocation across the cytoplasmic membrane, allowing *R. rubrum* to grow with CO as its sole energy source [4].

The three-dimensional molecular structure of CO-treated CODH from *R. rubrum* has been solved at a 2.8-Å resolution [2]. The structure of the active-site C-cluster of CODH is shown in Fig. 1. The molecular

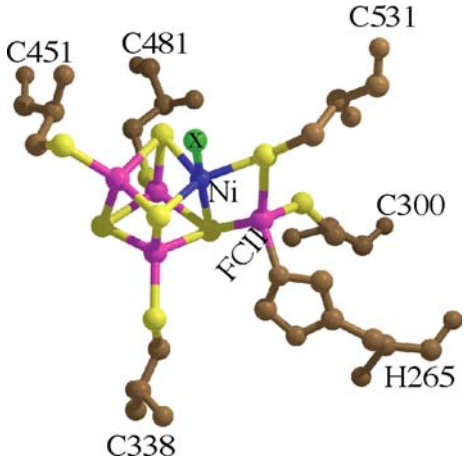

Fig. 1 Model of the three-dimensional molecular structure of the C-cluster from *Rhodospirillum rubrum* carbon monoxide dehydrogenase (*CODH*). The [$NiFe_4S_4$] cluster (or C-cluster) of *R. rubrum* is coordinated by residues His265, Cys300, Cys338, Cys451, Cys481, and Cys531 of CODH. The Ni atom is an integral part of a [$NiFe_3S_4$] cubane that is linked to a mononuclear Fe atom (*FCII*). Fe atoms are colored in *magenta*, sulfur atoms in *yellow*, Ni atom in *blue*, and the ligand to the Ni atom (presumably CO) is in *green*. All other atoms are in *brown*

structures of the C-clusters from *Carboxydothermus hydrogenoformans* CODHII and *Moorella thermoacetica* acetylcoenzyme A synthase/CODH have also been determined and are similar to the structure of the C-cluster of *R. rubrum* [5, 6]. The C-cluster consists of a nearly cubic [$NiFe_3S_4$] subcluster and an external Fe atom known as the ferrous component II site (FCII). In *R. rubrum* CODH, amino acid residues Cys338, Cys451, and Cys481 coordinate the iron atoms of the [$NiFe_3S_4$] subcluster. The nickel atom at one corner of the cubane is coordinated by two μ^2-bridging sulfides, one μ^3-bridging sulfide, one unidentified non-protein ligand (presumably CO), and the thiolate of Cys531. The FCII is coordinated by residues His265, Cys300, and one μ^3-bridging sulfide from the [$NiFe_3S_4$] subcluster. The Ni atom and the FCII site are bridged by the thiolate of Cys531.

When *R. rubrum* is grown under CO with Ni-depleted media, an inactive CODH is formed [7, 8]. This inactive CODH (hereafter referred to as apo-CODH) lacks Ni but retains the full complement of Fe found in CODH. Ni can be inserted into the vacant Ni site of apo-CODH to reconstitute the C-cluster and the CODH activity. Variation of the amino acid ligands to the C-cluster by site-directed mutagenesis of the gene encoding for CODH, *cooS*, produces CODHs that have low CO oxidation activity and altered spectroscopic properties [9, 10]. These variants have provided key insights into the electronic properties of the C-cluster. Previous work has concentrated on the two amino acid residues, Cys531 and His265, directly bound to the Ni and FCII atoms of the C-cluster. This subcluster is proposed to be the site of CO oxidation. In this work, we constructed site-directed variants of amino acid ligands bound to the 3Fe portion (C338A, C451A, C451S, C481A) of the C-cluster to observe the effects of these amino acid variations on the function and assembly of the C-cluster. Analyzing these new variants as well as C531A CODH, we propose a model mechanism for Ni insertion into the active-site C-cluster.

Materials and methods

Materials and buffers

All glassware used to prepare culture medium, for cell growth, and for activity assays was washed with 4 N HCl and rinsed thoroughly with metal-free deionized water. One hundred millimolar 3-(*N*-morpholino)propane sulfonate (MOPS), 2-(*N*-morpholino)ethanesulfonic acid (MES), and 2-(cyclohexylamino)ethanesulfonic acid (CHES) buffers were made metal-free by passage through a column of Chelex-100 cation-exchange resin (Bio-Rad). Metal-free buffers were used during protein purification, enzyme assays, and Ni activation assays. All purification steps and assays were performed under anaerobic conditions using buffers containing 1 mM sodium dithionite (DTH) or inside a Vacuum Atmosphere anaerobic glove box (model HE-493; Hawthorne, CA, USA).

Site-directed mutagenesis of *cooS*

Site-directed mutagenesis of *cooS* was performed as previously described by using plasmid pCO11 as a template and either the restriction-site elimination method or the QuickChange method (Stratagene) [9, 11]. The presence of the mutations introduced was confirmed by sequencing. Standard media, antibiotic usage, and mating protocols were employed [12]. The *R. rubrum* strains expressing CODH variants used in this work were UR2 (wild type), UR731 (C338A), UR614 (C451A), UR859 (C451S), UR498 (C481A), and UR502 (C531A, described in Ref. [10]).

In vivo ^{63}Ni accumulation on CODH

R. rubrum strains were grown under photoheterotrophic conditions in 2 ml Ni-free malate–ammonium (MN) medium. CODH synthesis was induced when the culture reached an OD_{600} of 1.0–1.5 by adding CO (20% gas phase) and $^{63}NiCl_2$ (0.6 μM final concentration; specific activity 9.8 mCi mg^{-1}) [13]. When the OD_{600} of the culture reached 4.0, cells were harvested by centrifugation and were washed with 100 mM MOPS buffer (pH 7.5) to remove ^{63}Ni bound nonspecifically to the cell surface. The cells were resuspended in 5 ml MOPS buffer and disrupted by osmotic shock. After centrifugation at 15,000*g* for 10 min, the pellet fraction was resuspended in MOPS buffer and subjected to heat

treatment at 60 °C for 3 min. Precipitated materials were removed by centrifugation at 15,000 *g* for 10 min. The CODH-containing supernatant fraction was subjected to sodium dodecyl sulfate polyacrylamide gel electrophoresis (SDS-PAGE) for 2 h at 100 V. After electrophoresis, the gel was dried and exposed to a PhosphorImager screen for 3–7 days. The screens were analyzed using a Molecular Dynamics model 425e PhosphorImager.

Purification of wild-type and mutated forms of CODH

Cells were grown on either Ni-free or Ni-supplemented (50 μM $NiCl_2$) MN medium as previously described [7, 14]. Wild-type and variant CODHs were purified according to established procedures [14, 15].

On-column incorporation of Ni by CODH

On-column Ni incorporation into wild-type and variant forms of apo-CODH was performed according to the method of Heo et al. [15]. Apo-CODH samples were loaded onto a (diethylamino)ethyl (DEAE) cellulose DE-52 column (5-ml bed volume) and washed with 20 ml of 100 mM MOPS buffer (pH 7.5). Apo-CODH on the column was then treated with either CO-saturated or CO-free 100 mM MOPS buffer (pH 7.5). Ni incorporation into apo-CODH was performed by applying 10 ml of 100 mM MOPS buffer (pH 7.5) supplemented with 5 mM $NiCl_2$ and 0.1 mM DTH to the column-bound protein. Nonspecifically bound Ni was removed by washing the column with 50 ml of 100 mM MOPS buffer (pH 7.5). CODH samples were eluted from the DE-52 resin with 100 mM MOPS containing 400 mM of NaCl, and were subsequently desalted by passage through a Sephadex G-25 column (0.5 cm×10 cm) equilibrated in 100 mM MOPS buffer (pH 7.5).

Electron paramagnetic resonance analysis of C451S CODH

Purified C451S CODH (71 units mg^{-1}, 2.8 mg ml^{-1}) was desalted by passage through a Sephadex G-25 column (0.5 cm×10 cm) equilibrated in 100 mM MOPS buffer (pH 7.5) to remove DTH. The desalted protein was placed in electron paramagnetic resonance (EPR) tubes in 250-μl portions. The samples were treated as described in the "Results." The redox potential of the dyes was determined by monitoring the appropriate absorption in the visible spectrum for indigo carmine [$\lambda_{max} = 610$ nm (oxidized), $\varepsilon = 19.9$ mM^{-1} cm^{-1}] and phenosafranin [$\lambda_{max} = 518$ nm (oxidized), $\varepsilon = 25.7$ mM^{-1} cm^{-1}]. The final concentration of the redox dyes in the EPR samples was 100 μM. EPR was performed at a microwave frequency of 9.44 GHz and a modulation amplitude of 10 G using a Bruker ESP 300E EPR spectrometer equipped with a Bruker ER0815 frequency converter, a Bruker ER041 XG microwave bridge, and an Oxford ITC temperature controller.

Kinetics analysis of CODH activation by Ni

Apo-CODH activation by Ni follows pseudo-first-order kinetics. The apparent first-order rate constant (k_{obs}) for Ni activation was determined at different concentrations of $NiCl_2$ [8]. The saturable nature of the activation implies a two-step mechanism in which the enzyme reversibly binds Ni to form an inactive complex, which is then irreversibly activated (Scheme 1).

$$\mathrm{E} + \mathrm{Ni} \underset{k_2}{\overset{k_1}{\rightleftharpoons}} \mathrm{E{\bullet}Ni} \xrightarrow{k_{max}} \mathrm{E{\bullet}Ni^*}$$

Scheme 1

The dissociation constant ($K_D = k_2/k_1$) for Ni and the maximal rate constant for activation (k_{max}) were calculated using the equation

$$k_{obs} = \frac{k_{max}[\mathrm{Ni}]}{K_D + [\mathrm{Ni}]}. \quad (1)$$

pH dependence of apo-CODH activation by Ni

Activation mixtures contained 1 ml metal-free CO-saturated 100 mM buffer, 0.2 μM methyl viologen, 5 mM $NiCl_2$, and traces of DTH. The buffers used were MES (pH 6.0–6.5), MOPS (pH 7.0–8.0), and CHES (pH 8.5–9.5). Ni activation was initiated by adding apo-CODH into the reaction mixture. Five-microliter aliquots were withdrawn from the activation mixture at 5-min intervals and assayed for CO oxidation activity. As control reactions, apo-CODH samples were preincubated for 30 min in the same range of pH but Ni activation was performed in MOPS buffer at pH 7.5. This pretreatment did not change the specific activity obtained after Ni activation. Both wild-type and mutant forms of apo-CODH were found to be stable for at least 30 min in the pH range from 6.5 to 9.5. The pH-dependence plots were fit assuming the presence of two pK_a values (pK_{a1} and pK_{a2}) and a single k_{max} according to Ref. [16] and the equation

$$k_{obs} = \frac{k_{max}K_{a1}[\mathrm{H}^+]}{(K_{a1} + [\mathrm{H}^+])(K_{a2} + [\mathrm{H}^+])}. \quad (2)$$

Protein assays and metal analysis

SDS-PAGE was performed according to the method of Laemmli [17]. Polyclonal anti-CODH antibodies were

raised in rabbits at the Polyclonal Antibody Service of the University of Wisconsin-Madison. Western blots were performed as previously described [18]. Quantitative immunoblotting was conducted using ^{63}Ni-labeled CODH as a standard [19]. Protein concentrations were determined by the bicinchoninic acid method using bovine serum albumin as a standard [20]. Protein metal content was determined by inductively coupled plasma mass spectrometry at the University of Georgia Chemical Analysis Laboratory.

CODH activity assay

CO oxidation activity was assayed at room temperature by following the reduction of methyl viologen at 578 nm ($\varepsilon = 9.7\ mM^{-1}\ cm^{-1}$) in CO-saturated metal-free 100 mM MOPS buffer (pH 7.5) containing 10 mM methyl viologen and 2 mM EDTA [8]. CODH specific activity is expressed as micromoles of CO oxidized per minute per milligram of protein.

Ni activation assay

Ni activation of apo-CODH in the absence of CO was performed as previously described [8, 19]. Ni activation in the presence of CO was carried out by incubating the apo-CODH in CO-saturated 100 mM MOPS buffer (pH 7.5) containing 5 mM $NiCl_2$, 0.2 mM methyl viologen, and trace amounts of DTH at 25 °C. Five-microliter aliquots of the activation mixture were removed every 5 min and CODH activity was assayed as CO-dependent methyl viologen reduction.

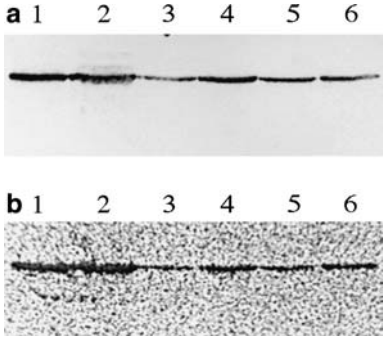

Fig. 2 In vivo ^{63}Ni accumulation into variant forms of CODH. **a** Western blot analysis of the membrane fractions from *R. rubrum* wild-type and variant strains developed with antibodies to CODH. **b** Phosphorimage analysis of the in vivo ^{63}Ni incorporation into wild-type and variant forms of CODH. Proteins from cell-free extracts were separated by sodium dodecyl sulfate polyacrylamide gel electrophoresis. CODH levels were estimated by quantitative immunoblotting with ^{63}Ni-labeled CODH as a standard. Note that different amounts of protein were loaded in each lane. *Lane 1* wild-type strain (UR2, 73 μg total protein), *lane 2* C338A (UR731, 78 μg total protein), *lane 3* C451A (UR614, 21 μg total protein), *lane 4* C451S (UR859, 45 μg total protein), *lane 5* C481A (UR498, 32 μg total protein), *lane 6* C531A (UR502, 37 μg total protein)

Results

Variations to ligands of the 3Fe portion of the C-cluster do not support CO-dependent growth of *R. rubrum*

Unlike the wild-type strain UR2, *R. rubrum* strains with variations at residues Cys338 (C338A), Cys451 (C451A, C451S), and Cys481 (C481A) of CODH were unable to grow anaerobically in the dark with CO as the energy source. To establish whether the failure of these strains to grow on CO was due to CODH protein instability or to the inability of the CODH variants to interact with the cytoplasmic membrane, their membrane fractions were isolated and analyzed by Western blot with antibodies to CODH. Membrane association of CODH is required to couple CO oxidation to H_2 evolution by the CO-induced hydrogenase [3]. Figure 2a shows that the amount of CODH present in the membrane fraction of *R. rubrum* (relative to the amount of protein loaded) was similar in the wild-type and variant strains, indicating that single variations of cysteine ligands to the C-cluster do not cause in vivo CODH instability or inhibit membrane association.

CODH variants accumulate wild-type levels of ^{63}Ni in vivo

Substitution of the cysteine residues that coordinate the C-cluster may affect the ability to incorporate Ni into CODH. To test this possibility, in vivo ^{63}Ni-radio labeling experiments were performed as described in the "Materials and methods" section. The membrane fractions from *R. rubrum* strains grown in medium containing ^{63}Ni were isolated, subjected to SDS-PAGE, transferred to a nitrocellulose membrane, and analyzed using a PhosphorImager system (Fig. 2b). The quantification of ^{63}Ni label on CODH using a standard of purified ^{63}Ni-CODH showed that all variant forms of CODH contained approximately 0.9 mol ^{63}Ni per mole of CODH monomer, which is similar to the level observed for the wild-type CODH. This result clearly indicates that cysteine residues 338, 451, 481, and 531 are not individually essential to accumulate Ni into CODH. These results are also consistent with previous metal analysis of purified C531A CODH [10].

Purification of CODH variants

Wild-type, C338A, C451A, C451S, C481A, and C531A CODH variants were purified from the *R. rubrum* mutant strains UR2, UR731, UR614, UR859, UR498, and UR502, respectively. All purification steps were performed under anaerobic conditions and using metal-free buffers to avoid oxidative degradation and metal contamination. CODH variants behaved like the wild-type enzyme in all purification steps with the exception of

Table 1 Metal contents and specific activities of purified carbon monoxide dehydrogenase (*CODH*) variants

CODH variant[a]	Metal content[b] [mol (mol CODH)$^{-1}$]		Specific activity [μmol CO oxidized (min mg CODH)$^{-1}$]
	Ni	Fe	
Wild type	0.85 ± 0.05	8.97 ± 0.1	6,230 ± 74.9
C338A	0.87 ± 0.06	7.29 ± 0.3	< 0.1
C451A	0.92 ± 0.08	6.58 ± 0.7	< 0.1
C451S	0.84 ± 0.09	7.59 ± 0.7	86.3 ± 7.5
C531A	0.85 ± 0.05[c]	8.9 ± 0.1[c]	6.9 ± 1.8

[a]All CODH variants were purified from *Rhodospirillum rubrum* cells grown on malate–ammonium medium supplemented with 50 μM $NiCl_2$

[b]Metal content and specific activity were determined as described in "Materials and methods." The values represent means ± standard deviations of at least five independent experiments

[c]The values were taken from Ref. [10]

heat treatment. About 40% activity of the C338A, C451A, or C451S CODH variants was recovered following heat treatment compared with the 60% yield reported for wild-type CODH, suggesting that the CODH variants with ligand substitutions to the C-cluster are less stable than wild-type CODH [15]. In particular, the C481A variant was so unstable that we were unable to recover useable amounts after heat treatment. The typical yield for the purification of the CODH variants was approximately 0.26 mg of protein per gram of cell paste.

The metal content and enzymatic activity of the CODH variants were determined and compared with those of the wild-type enzyme (Table 1). CO oxidation activity was greatly impaired in all CODH variants. The specific activities of C451S and C531A variants were 1.4 and 0.1% of the wild-type values, respectively; the C338A and C451A variants were inactive. Previous metal analyses of wild-type CODH gave 0.8–1.0 atoms of Ni and 8–9 atoms of Fe per monomer [21, 22]. All CODH variants contained the same amount of Ni as the wild type. This result is consistent with the observed in vivo ^{63}Ni accumulation on CODH variants as determined by phosphorimage analysis (see before). Table 1 shows that the C531A variant also possesses wild-type levels of Fe, as previously reported [10]. Metal analysis indicated that C338A, C451A, and C451S variants contained approximately seven Fe atoms per CODH monomer, suggesting the metal clusters of these variants may be more labile.

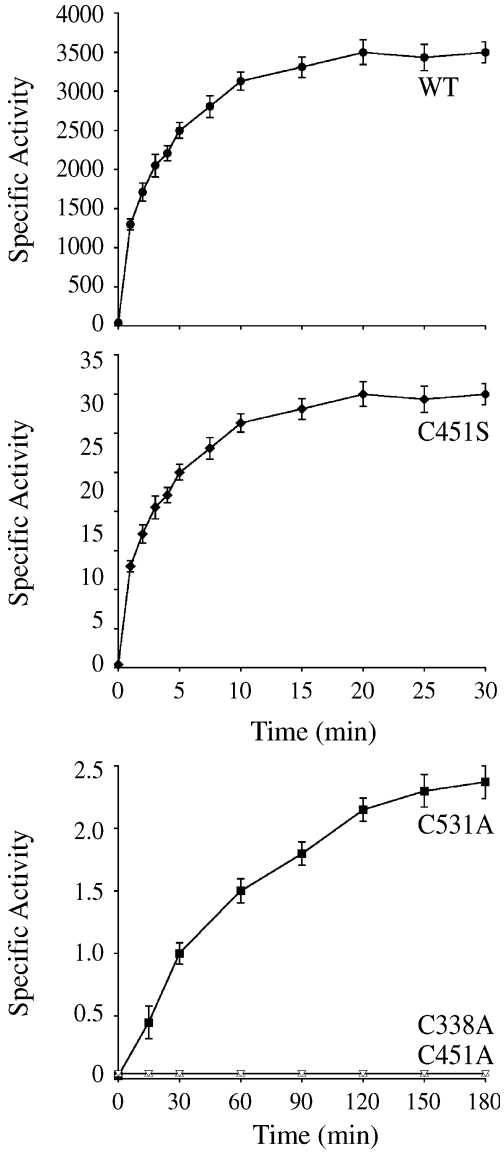

Fig. 3 In vitro activation of CODH variants by Ni. The CODH variants are wild type (*WT*), *C338A* (*up triangles*), *C451A* (*inverted triangles*), *C451S*, and *C531A*. Ni activation was initiated by adding 20 μg of pure apo-CODH variant to a CO-saturated activation mix containing 100 mM 3-(*N*-morpholino)propanesulfonate (*MOPS*) (pH 7.5), 5 mM $NiCl_2$, 0.2 mM methyl viologen, and trace amounts of sodium dithionite (*DTH*). At the indicated time points, 5-μl aliquots were removed and CODH activity was determined as CO-dependent methyl viologen reduction. Treatment of apo-C338A and C451A CODH variants with 5 mM $NiCl_2$ did not produce any detectable activity. Specific activities are given in micromoles of CO oxidation per minute per milligram of CODH

Ni activation of apo-CODH variants

The apo-CODH variants C338A, C451A, C451S, and C531A were purified from *R. rubrum* cells grown on Ni-free MN medium. Metal analysis indicated that all apo-CODH variants contained less than 0.05 mol of Ni per mole of CODH monomer. The ability of variant CODHs to incorporate Ni into the active site in vitro was examined by incubating the purified apo-CODH variants with Ni under reducing conditions and determining the CO oxidation activity of the reconstituted CODHs (Fig. 3). A reaction containing wild-type apo-CODH was included as a control and showed that the enzyme activity increased to a maximum of 3,500 units mg^{-1} of protein after 15 min of activation. Apo-C451S CODH was activated to

31 units mg^{-1} of protein and reached a plateau after 15 min. The activation of apo-C531A CODH was much slower and did not reach a plateau after 3 h of incubation with Ni. No activation of apo-C338A CODH or C451A CODH was observed in a reaction time of 3 h, which is consistent with the absence of CODH activity in the Ni-containing forms of these variants (Table 1).

To determine the amount of Ni incorporated into the CODH variants during the reconstitution, apo-CODH variants were bound to a DEAE cellulose resin, incubated with buffer containing 5 mM $NiCl_2$, washed with metal-free buffer to remove nonspecifically bound Ni, and eluted in metal-free buffer supplemented with 400 mM NaCl. Metal analysis of the samples eluted indicated that all CODH variants (C338A, C451A, C451S, C531A) contained approximately 0.9 mol of Ni per mole of CODH monomer (data not shown).

Detailed characterization of C451S CODH

Since C451S CODH was the CODH variant studied here that possessed more CO oxidation activity, its biochemical properties were investigated in detail. As noted before, C451S CODH has 1.4% of the CO oxidation activity of wild-type CODH. However, the K_M of C451S CODH for CO was 24 μM, which is very similar to the K_M for CO of wild-type CODH (32 μM), indicating that CO can bind to the altered C-cluster as well as to the C-cluster of wild-type CODH [15]. Absorbance measurements of C451S CODH at 420 nm yielded extinction coefficients for thionin-oxidized samples (33 mM^{-1} cm^{-1}) and DTH-reduced samples (20 mM^{-1} cm^{-1}) that were very similar to extinction coefficients measured for wild-type CODH [14]. These measurements suggest that the same number of Fe–S clusters are present in C451S CODH and wild-type CODH.

The electronic properties of the metal clusters of C451S CODH were investigated by EPR spectroscopy. Wild-type CODH has three diagnostic EPR active states: C_{red1} ($g_{avg} = 1.87$), a rhombic signal arising from the C-cluster which has $E_o = -110$ mV, B_{red}($g_{avg} = 1.94$), a rhombic signal arising from the reduced B-cluster which has $E_o = -418$ mV, and C_{red2}($g_{avg} = 1.89$), a rhombic signal arising from the C-cluster when CODH is reduced with CO or DTH [21, 23]. When C451S CODH was treated with 50% reduced indigo carmine (−175 mV at pH 7.5) or 50% phenosafranin (−302 mV at pH 7.5), no EPR signal was observed. Under these conditions, the C_{red1} signal observed for wild-type CODH is readily generated [21, 23]. When C451S CODH was treated with 2 mM DTH, EPR signals were observed that had the same g value as the B_{red} and C_{red2} signals observed for wild-type CODH (Fig. 4). As observed for wild-type CODH, C_{red2} was maximized at 4.5 K and absent at 20 K; the B_{red} signal relaxes more slowly than C_{red2} and was observable at 20 K. Another difference between wild-type CODH and C451S CODH was that the C_{red2} signal, in particular the $g_x = 1.76$ component, appeared broader in the EPR spectrum of C451S CODH.

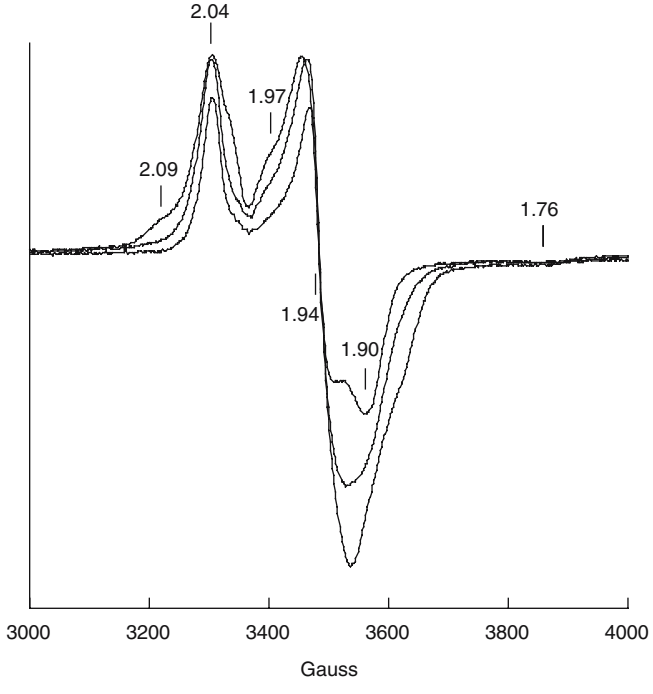

Fig. 4 Electron paramagnetic resonance (*EPR*) spectra of C451S CODH (2.8 mg ml^{-1}) reduced with 2 mM DTH. Spectra were recorded at 4.5, 10, and 20 K and 10-mW microwave power. Sample preparations and EPR setup are described in "Materials and methods"

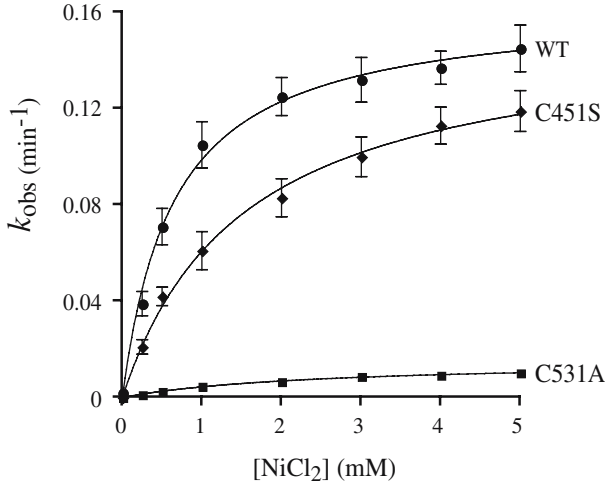

Fig. 5 Dependence of the apparent first-order rate constant (k_{obs}) of CODH activation on Ni concentration. The values of k_{obs} for the activation of wild-type (*WT*), *C451S*, and *C531A* CODH variants were determined at different Ni concentrations as described in "Materials and methods." The *lines* represent the fit of the experimental data to Eq. 1. K_D and k_{max} values were derived from the fits and are listed in Table 2

Table 2 Kinetics parameters and pK_a values for the activation by Ni of wild-type, C451S, and C531A CODH variants

CODH variant	$K_{D\ Ni}$ (mM)	k_{max} (min^{-1})	k_{max}/K_D	pK_{a1}[a]	Optimum pH	pK_{a2}	Specific activity[b]
Wild type	0.65 ± 0.11	0.163 ± 0.005	0.250	7.6 ± 0.1	8.6	9.5 ± 0.2	3,501 ± 137
C451S	1.53 ± 0.12	0.154 ± 0.007	0.100	7.1 ± 0.1	8.4	9.5 ± 0.2	31.1 ± 2.5
C531A	1.95 ± 0.31	0.014 ± 0.002	0.007	–[c]	–	–	2.4 ± 0.1

CODH activation by Ni was performed at 20 °C in CO-saturated metal-free buffers as described in "Materials and methods." The apparent first-order rate constants (k_{obs}) were determined for $NiCl_2$ concentrations in the range from 0.1 to 5 mM. The K_D for Ni and k_{max} of activation were calculated by applying Eq. 1 to the curve fitting the data represented in Fig. 5. The values are the averages ± standard deviations of at least five independent experiments

[a] pK_a values were determined assuming the presence of two pK_a values and a single k_{max}

[b] Specific activities are given in micromoles of CO oxidized per minute per milligram of CODH

[c] The activation profile of C531A is independent of pH in the 6.5–9.5 range

Kinetics of Ni insertion into C-cluster variants

CO oxidation activities of several CODH variants with substitutions of C-cluster ligands have been reported before. However, the activation of apo-CODH variants by Ni was not studied. The availability of stable, apo-CODH C-cluster variants allowed us to examine the kinetics of Ni activation and to determine the effect of ligand substitution. Since C451S CODH has residual CODH activity, kinetics of Ni activation were compared directly with Ni activation kinetics of wild-type CODH. Kinetics of Ni activation of apo-C531A CODH were also measured to compare the effect of ligand substitution directly to the Ni atom in the C-cluster with substitution of a ligand to the 3Fe portion of the C-cluster. The data shown in Fig. 3 were used to calculate the apparent first-order rate constant (k_{obs}) of CODH activation at a given Ni concentration. Different k_{obs} were obtained by changing the concentration of Ni in the activation assay. In wild-type, C451S, and C531A CODH variants, k_{obs} depended on Ni concentration and a plot of k_{obs} versus Ni concentration had a hyperbolic saturation profile (Fig. 5). The activation kinetics observed in this work agree with previous results and support the proposed model of a rapid formation of a Ni•CODH complex followed by a rate-determining conversion to an active CODH [8].

Affinity for Ni (K_D) and the maximum activation rate constants (k_{max}) for the wild-type, C451S, and C531A CODH variants were derived from plots of k_{obs} versus Ni concentration (Table 2). C451S exhibited a 2.4-fold increase in K_D and a 1.1-fold decrease in k_{max} compared with the wild-type CODH. In contrast, the C531A variant exhibited a 3.0-fold increase in K_D but a 11.6-fold decrease in k_{max} compared with the wild-type CODH. The k_{max}/K_D ratio for C451S and C531A variants was reduced by 2.5-fold and 35.7-fold, respectively, when compared with that for the wild-type CODH.

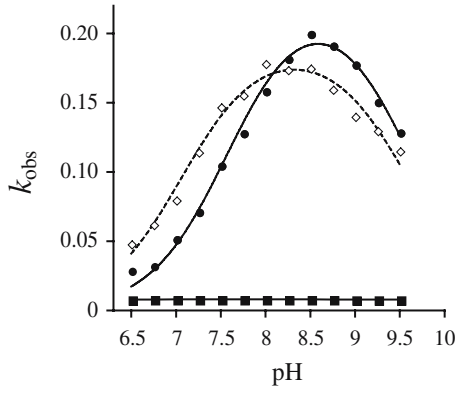

Fig. 6 Dependence of k_{obs} for CODH activation on pH. The values of k_{obs} (in units of per minute) for the activation by Ni of wild-type (*circles*), C451S (*diamonds*), and C531A (*squares*) CODH variants were determined at 25°C in CO-saturated 100 mM 2-(*N*-morpholino)ethanesulfonic acid (pH 6.0–6.5), MOPS (pH 7.0–8.0), or 2-(cyclohexylamino)ethanesulfonic acid (pH 8.5–9.5) buffer supplemented with 5 mM $NiCl_2$, and 0.2 mM methyl viologen. The *lines* for wild-type CODH and C451S CODH represent the fit of the experimental data to Eq. 2 (see "Materials and methods"). pK_a values were derived from the fits and are listed in Table 2. The C531A CODH data do not fit well to Eq. 2 (data not shown)

Analysis of the pH dependence of CODH activation by Ni

The kinetics studies of Ni activation suggested that Cys531 was a critical residue for the efficient insertion of Ni into CODH. To elucidate the mechanism of this process in greater depth, we examined the dependence of Ni activation on pH. The k_{obs} values for Ni activation were measured over the pH range 6.5–9.5 for wild-type CODH and the dependence of k_{obs} on pH was fitted to a bell-shaped curve with a maximum k_{obs} of 0.2 min^{-1} at pH 8.6 and two pK_a at 7.6 and 9.5 (Fig. 6, Table 2). The pH-dependent k_{obs} profile for C451S activation was similar to that of the wild type, showing a slight decrease (0.2–0.4 units) in the values of pK_{a1} and the optimum pH of activation and no change in pK_{a2} (Fig. 6, Table 2). The large effect of the C531A substitution on the activation k_{max} (see before) prompted us to test whether one or both of the pK_a values observed in the pH-dependent k_{obs} profile depend on Cys531. Surprisingly, the apparent activation rates of C531A were found to be pH-independent (Fig. 6).

Discussion

Cysteine ligands to the [Fe_3S_4] subcluster are critical for CODH activity but not for C-cluster formation

The four new CODH variants (C338A, C451S, C451A, C481A) described in the earlier sections exhibited little or no CO oxidation activity. Previous studies had shown that substitutions of Cys531 and His265 also caused substantial decreases in CO oxidation activity [9, 10]. These results establish that the cysteine and histidine ligands to the C-cluster are critical for efficient catalysis. All of the residues that provide ligands for the C-cluster, except for Cys300, are strictly conserved among CODHs identified by sequence comparisons [1]. Despite the loss of CO oxidation activity of the CODH variants, the altered C-clusters of these variants appear to be intact and competent for Ni binding. The in vivo ^{63}Ni labeling experiments clearly show that all the CODH variants accumulate levels of Ni similar to the level in wild-type CODH. CODHs from three of the variants (C451A, C451S, C338A) were stable enough to be purified in significant amounts. Metal analysis of the purified CODH variants indicated that the levels of Ni in the purified proteins did not decrease compared with the levels in the in vivo labeling studies, showing that Ni is stably bound to the protein through multiple purification steps, including heat treatment at 80 °C. The levels of Fe for the purified CODH variants are slightly lower than the levels observed for wild-type and C531A CODH, but are consistent with the majority of the purified proteins having intact Fe–S clusters. Furthermore, the apo forms of the variant CODHs are all capable of incorporating approximately one Ni atom per CODH monomer when Ni is inserted by on-column activation. These results indicate the C-cluster is preorganized to bind Ni and substitution of the ligands to the C-cluster does not substantially affect the Ni binding site. One interesting aspect of the properties of the C-cluster is that the H265V CODH variant shows altered Ni binding. This is puzzling because residue His265 in wild-type CODH binds FCII rather than Ni [9]. Purified H265V CODH has low levels of Ni (0.24 Ni atoms per CODH monomer) despite being isolated from cells grown on 50 μM $NiCl_2$. When the "as-purified" H265V CODH was incubated with 5 mM $NiCl_2$, 2.4 Ni atoms were incorporated into CODH, indicating the protein contains more than one binding site for Ni. Comparison with the current work indicates that His265 is the only critical residue required for proper assembly of the Ni binding site for the C-cluster. The mechanism by which His265 directs assembly of the C-cluster is unknown and is under active investigation.

The insensitivity of the C-cluster of *R. rubrum* to most ligand substitutions differs from results obtained for related biological Ni-containing metalloclusters. Friedrich and Maasanz [24] found that variation of the cysteine ligands that bind the Ni atom in the active site of the NAD^+-reducing [NiFe] hydrogenase from *Alcaligenes eutrophus* afforded inactive enzymes that were unable to bind Ni and unable to form the oligomeric structures required for catalysis.

Mechanism of Ni activation of apo-CODH

The residual CO oxidation activity measured for C451S CODH allowed us to investigate the mechanism of Ni

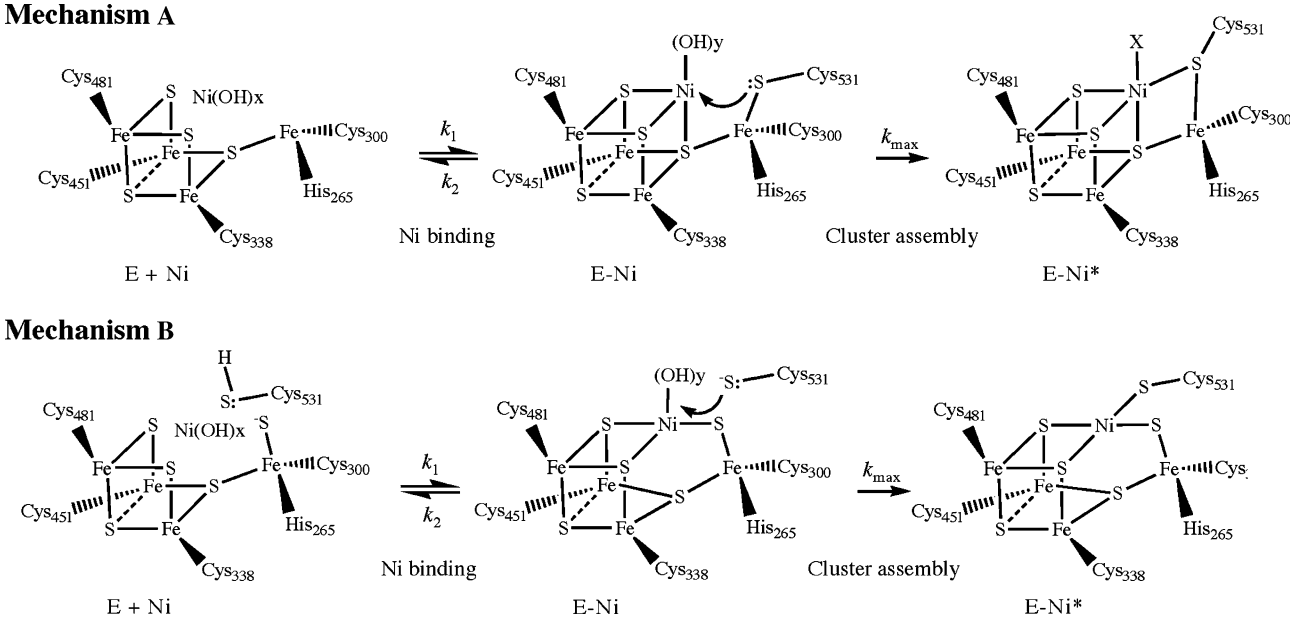

Fig. 7 Proposed models for the mechanism of Ni insertion into apo-CODH. In *mechanism a*, the structure of the mature [$NiFe_4S_4$] C-cluster of *R. rubrum* CODH is adapted from Ref. [2]. In *mechanism b*, the structure of the mature [$NiFe_4S_4$] C-cluster of *R. rubrum* CODH is adapted from Refs. [5, 6]. Ligand *X* is presumed to be CO

insertion into apo-CODH using the in vitro reconstitution assay. Spectroscopic studies of C451S CODH revealed that it had similar absorbance and EPR spectra to wild-type CODH. However, the substitution causes sufficient perturbation of the C-cluster to remove the electronic state giving rise to the C_{red1} EPR signal, and to cause a more than 50-fold decrease in catalytic activity. The similarity of the spectroscopic features between C451S CODH and wild-type CODH prompted us to examine if there were any differences in the kinetics of Ni insertion into the apo proteins. Ni insertion into apo-C531A CODH was also examined because previously reported spectroscopic studies on this variant had shown markedly different C-cluster signals in comparison with wild-type CODH. The primary effect of the C451S substitution on the kinetics of activation is a 2.4-fold decrease in Ni affinity. The change in Ni affinity for C451S CODH is relatively small and it seems reasonable that subtle variations in the environment around the Ni binding site could produce such variations. Apo-C531A CODH is mainly affected in the maximum rate of activation (k_{max}), which is 12-fold lower than in wild-type apo-CODH. Conversion from the inactive to the active Ni•CODH complex is the rate-limiting step of the Ni activation process and it is quantified by k_{max}. Taken together, our results suggest that the $[Fe_3S_4]$ subcluster binds Ni and the thiolate group of Cys531 converts the inactive Ni•CODH complex to the C-cluster. The kinetics results also suggest that the residual activation of C531A by Ni occurs by a different mechanism.

The effect of pH on the rate of Ni activation of wild-type apo-CODH is consistent with the deprotonation ($pK_{a1} = 7.6$) and protonation ($pK_{a2} = 9.5$) of two groups during Ni insertion. The pK_a values derived from the pH-dependent k_{obs} profile of C451S are similar to those of wild-type CODH, indicating Ni is inserted by a similar mechanism. However, C531A exhibits a pH-independent k_{obs} profile, strongly suggesting that pK_{a1} arises from the deprotonation of the thiol group of Cys531. A pK_{a1} of 7.6 is lower than the value of 8.4 expected for thiol/thiolate equilibrium in free cysteine, but is consistent with the deprotonation of a metal-assisted cysteine residue [25]. The coordination of Cys531 to the Fe atom of the FCII site may increase the acidity of the thiol proton of Cys531 and facilitate formation of a μ^2-bridged Fe–S–Ni bond. The origin of pK_{a2} is more difficult to assign, as it also disappears in C531A. One possibility is that pK_{a2} arises from a group involved in the stabilization of the thiolate of Cys531. One likely candidate is the amino group of Lys568 that is in hydrogen-bonding distance to the thiol group of Cys531 and that would be protonated under physiological conditions [2].

On the basis of mechanistic studies of Ni activation and of the X-ray crystal structure of *R. rubrum* CODH, the following mechanism for Ni insertion into apo-CODH is proposed (Fig. 7, mechanism a). Three sulfide atoms from the dithionite-reduced $[Fe_3S_4]$ subcluster bind Ni to form an initial Ni•CODH complex. The Ni binding may be redox-dependent, because apo-CODH does not undergo Ni insertion at redox potentials above −350 mV. The Fe atom of the FCII site facilitates the deprotonation of the thiol group of Cys531, which then binds to Ni to complete C-cluster assembly.

An alternative mechanism for Ni insertion based on the C-cluster structure obtained for *C. hydrogenoformans* CODHII is also proposed, since uncertainty exists about the catalytically active form of the C-cluster (Fig. 7, mechanism b) [26]. The major difference between the two structures is the presence of a μ^2-sulfide that bridges between the Ni and the FCII in the C-cluster from *C. hydrogenoformans* CODHII but is absent in the *R. rubrum* CODH. In this mechanism, Ni would bind reversibly to the two μ^2-sulfides of the $[Fe_3S_4]$ subcluster as well as to a terminal sulfide bound to FCII, followed by irreversible binding of the thiolate from Cys531 that would complete the C-cluster assembly.

Acknowledgements We thank Robert L. Kerby for providing us with the *cooS* site-directed mutants used in this study. We thank Steve Cramer and Simon George of Lawrence Berkeley National Laboratory for use of their EPR spectrometer. We also thank Jongyun Heo for preliminary characterization of some of the CODH variants described here. This work was supported by US Department of Energy Basic Energy Sciences grant DE-FG03–03ER15383 to P.W.L.

References

1. Lindahl PA (2002) Biochemistry 41:2097–2105
2. Drennan CL, Heo J, Sintchak MD, Schreiter E, Ludden PW (2001) Proc Natl Acad Sci USA 98:11973–11978
3. Ensign SA, Ludden PW (1991) J Biol Chem 266:18395–18403
4. Kerby RL, Ludden PW, Roberts GP (1995) J Bacteriol 177:2241–2244
5. Darnault C, Volbeda A, Kim EJ, Legrand P, Vernede X, Lindahl PA, Fontecilla-Camps JC (2003) Nat Struct Biol 10:271–279
6. Dobbek H, Svetlitchnyi V, Gremer L, Huber R, Meyer O (2001) Science 293:1281–1285
7. Bonam D, McKenna MC, Stephens PJ, Ludden PW (1988) Proc Natl Acad Sci USA 85:31–35
8. Ensign SA, Campbell MJ, Ludden PW (1990) Biochemistry 29:2162–2168
9. Spangler NJ, Meyers MR, Gierke KL, Kerby RL, Roberts GP, Ludden PW (1998) J Biol Chem 273:4059–4064
10. Staples CR, Heo J, Spangler NJ, Kerby RL, Roberts GP, Ludden PW (1999) J Am Chem Soc 121:11034–11044
11. Zhang YP, Burris RH, Ludden PW, Roberts GP (1996) J Bacteriol 178:2948–2953
12. Kerby RL, Ludden PW, Roberts GP (1997) J Bacteriol 179:2259–2266
13. Watt RK, Ludden PW (1999) J Bacteriol 181:4554–4560
14. Bonam D, Ludden PW (1987) J Biol Chem 262:2980–2987
15. Heo J, Staples CR, Halbleib CM, Ludden PW (2000) Biochemistry 39:7956–7963
16. Pearson MA, Park IS, Schaller RA, Michel LO, Karplus PA, Hausinger RP (2000) Biochemistry 39:8575–8584
17. Laemmli UK (1970) Nature 227:680–685
18. Blake MS, Johnston KH, Russell-Jones GJ, Gotschlich EC (1984) Anal Biochem 136:175–179
19. Jeon WB, Cheng JJ, Ludden PW (2001) J Biol Chem 276:38602–38609
20. Smith PK, Krohn RI, Hermanson GT, Mallia AK, Gartner FH, Provenzano MD, Fujimoto EK, Goeke NM, Olson BJ, Klenk DC (1985) Anal Biochem 150:76–85

21. Heo J, Staples CR, Telser J, Ludden PW (1999) J Am Chem Soc 121:11045–11057
22. Hu Z, Spangler NJ, Anderson ME, Xia J, Ludden PW, Lindahl PA, Münck E (1996) J Am Chem Soc 118:830–845
23. Spangler NJ, Lindahl PA, Bandarian V, Ludden PW (1996) J Biol Chem 271:7973–7977
24. Massanz C, Friedrich B (1999) Biochemistry 38:14330–14337
25. Rozema DB, Poulter CD (1999) Biochemistry 38:13138–13146
26. Dobbek H, Svetlitchnyi V, Liss J, Meyer O (2004) J Am Chem Soc 126:5382–5387